frontiers in Immunology

ORIGINAL RESEARCH
published: 27 January 2022
doi: 10.3389/fimmu.2022.803417

Deep Phenotypic Analysis of Blood and Lymphoid T and NK Cells From HIV+ Controllers and ART-Suppressed Individuals

Ashley F. George[1,2], Xiaoyu Luo[1], Jason Neidleman[1,2], Rebecca Hoh[3], Poonam Vohra[4], Reuben Thomas[5], Min-Gyoung Shin[5], Madeline J. Lee[6,7], Catherine A. Blish[6,7], Steven G. Deeks[3], Warner C. Greene[1,8], Sulggi A. Lee[9] and Nadia R. Roan[1,2]*

[1] Gladstone Institute of Virology, San Francisco, CA, United States, [2] Department of Urology, University of California San Francisco, San Francisco, CA, United States, [3] Division of HIV, Infectious Diseases and Global Medicine, University of California San Francisco, San Francisco, CA, United States, [4] Department of Pathology, University of California San Francisco, San Francisco, CA, United States, [5] Gladstone Institutes, San Francisco, CA, United States, [6] Department of Medicine, Stanford University School of Medicine, Stanford, CA, United States, [7] Program in Immunology, Stanford School of Medicine, Stanford, CA, United States, [8] Departments of Medicine, and Microbiology & Immunology, University of California San Francisco, San Francisco, CA, United States, [9] Zuckerberg San Francisco General Hospital and the University of California San Francisco, San Francisco, CA, United States*

OPEN ACCESS

Edited by:
Claudia Cicala, National Institute of Allergy and Infectious Diseases (NIH), United States

Reviewed by:
Lyle McKinnon, University of Manitoba, Canada
Alexandra Schuetz, US Army Medical Directorate of the Armed Forces Research Institute of Medical Sciences (USAMD), AFRIMS, Thailand

***Correspondence:**
Sulggi A. Lee
sulggi.lee@ucsf.edu
Nadia R. Roan
nadia.roan@gladstone.ucsf.edu

Specialty section:
This article was submitted to Viral Immunology, a section of the journal Frontiers in Immunology

Received: *28 October 2021*
Accepted: *04 January 2022*
Published: *27 January 2022*

Citation:
George AF, Luo X, Neidleman J, Hoh R, Vohra P, Thomas R, Shin M-G, Lee MJ, Blish CA, Deeks SG, Greene WC, Lee SA and Roan NR (2022) Deep Phenotypic Analysis of Blood and Lymphoid T and NK Cells From HIV+ Controllers and ART-Suppressed Individuals. Front. Immunol. 13:803417. doi: 10.3389/fimmu.2022.803417

T and natural killer (NK) cells are effector cells with key roles in anti-HIV immunity, including in lymphoid tissues, the major site of HIV persistence. However, little is known about the features of these effector cells from people living with HIV (PLWH), particularly from those who initiated antiretroviral therapy (ART) during acute infection. Our study design was to use 42-parameter CyTOF to conduct deep phenotyping of paired blood- and lymph node (LN)-derived T and NK cells from three groups of HIV+ aviremic individuals: elite controllers (N = 5), and ART-suppressed individuals who had started therapy during chronic (N = 6) vs. acute infection (N = 8), the latter of which is associated with better outcomes. We found that acute-treated individuals are enriched for specific subsets of T and NK cells, including blood-derived CD56-CD16+ NK cells previously associated with HIV control, and LN-derived CD4+ T follicular helper cells with heightened expansion potential. An in-depth comparison of the features of the cells from blood vs. LNs of individuals from our cohort revealed that T cells from blood were more activated than those from LNs. By contrast, LNs were enriched for follicle-homing CXCR5+ CD8+ T cells, which expressed increased levels of inhibitory receptors and markers of survival and proliferation as compared to their CXCR5- counterparts. In addition, a subset of memory-like $CD56^{bright}$TCF1+ NK cells was enriched in LNs relative to blood. These results together suggest unique T and NK cell features in acute-treated individuals, and highlight the importance of examining effector cells not only in blood but also the lymphoid tissue compartment, where the reservoir mostly persists, and where these cells take on distinct phenotypic features.

Keywords: HIV, lymph node, T cells, NK cells, CXCR5, controllers, CyTOF/mass cytometry

INTRODUCTION

Lymphocytes with cytotoxic capabilities, including both T and natural killer (NK) cells, are important effectors that play crucial roles in controlling infections by pathogenic viruses, including HIV. T cells include cytotoxic CD8+ T cells, which can directly kill HIV-infected cells, and CD4+ T cells, which can promote antibody responses, enhance CD8+ T cell responses, and directly implement cytotoxic effector functions. NK cells are similarly important in the antiviral immune response against HIV. These classical innate immune cells are rapidly mobilized to recognize and respond to viral infections in a manner regulated by a multitude of activating and inhibitory receptors, and can directly recognize and kill HIV-infected cells (1).

The activity of T and NK cells against HIV-infected cells is particularly important within lymphoid tissues, where the vast majority of the reservoir persists during antiretroviral therapy (ART) treatment (2). Because the follicles of lymphoid tissues appear to harbor a particularly dense array of HIV-infected cells (3–6), strategies are being developed to help direct cytotoxic CD8+ T cell and NK cell populations to this site (7, 8). These strategies include creating HIV/SIV-specific CAR (chimeric antigen receptor) T cells engineered to express CXCR5, a chemokine receptor mediating entry into the follicles (9, 10), or IL-15:IL-15Rα-based therapies, which upregulate CXCR5 in cytotoxic CD8+ T cells, thus facilitating their access to follicles (11, 12). People living with HIV (PLWH) harbor HIV-specific CXCR5+ CD8+ T cells both in circulation as well as within lymphoid tissues. These follicular HIV-specific T cells appear to have poor cytolytic activity compared to their blood counterparts (13, 14). Nonetheless, follicular CXCR5+ CD8+ T cells from LNs may contribute to viral control, since the viral load in PLWH correlates negatively with the frequency of these cells (13, 14). However, beyond the observation that these CD8+ T cells are poorly cytotoxic within the LNs, other features of these cells, and how LN-derived effector cells compare to blood-derived ones, are poorly understood.

NK cells, like CXCR5+ CD8+ T cells, may also be important in controlling HIV within B cell follicles. In SIV-infected African green monkeys that are able to control the infection without any treatment, lymphoid NK cells were largely CXCR5+ and persisted within the follicles of LNs (15). When NK cells were depleted in these animals *via* anti-IL-15 antibody, viremia increased in lymph nodes, suggesting an important role for follicular NK cells in viral control. In addition to classical innate responses, NK cells can also mount "memory" recall responses, including against HIV (16–19). One subset of memory-like NK cells, significantly increased in the peripheral blood of PLWH, was found to develop and expand in response to inflammatory cytokines, including IL-15 (19). This expansion was mediated by *TCF7* (transcript for TCF1), a transcriptional factor important for cellular quiescence and stemness (20, 21). Identified as CD94+*TCF7(TCF1)*+CD56^{bright} NK cells, these memory-like NK cells exhibit increased rates of proliferation and more robust effector functions in response to stimulation, and may aid in HIV control.

Unfortunately, both T and NK cells' effector responses often become dysfunctional upon HIV infection (22, 23), and do not completely recover even after ART treatment (24, 25), which historically has been initiated during the chronic phase of infection. However, there exists rare PLWH that can naturally control HIV in the absence of ART through immune-mediated mechanisms. These include elite controllers, who are thought to control the virus primarily through expression of specific class-I HLA alleles, which are able to elicit protective anti-HIV CD8+ T cell responses (26–31). More recently, post-treatment controllers (PTCs) have been described that exhibit durable control of HIV following withdrawal of ART. These individuals don't appear to express the protective class-I HLA alleles found in elite controllers (32), and may instead use NK cell-mediated mechanisms (33), which are understudied compared to T cell-mediated mechanisms. Interestingly, PTCs are over-represented among PLWH who initiate ART during acute infection (32, 34–36). In addition, PLWH who initiate ART during acute infection have lower levels of T cell activation (37) and a smaller HIV reservoir that decays more rapidly (38, 39), relative to those who initiated treatment during chronic infection. This is likely due to better preserved immune responses in these individuals (40–43). While early ART administration is now standard in the field, relatively little is known about the features of effector cells in these individuals and to what extent they may differ from those of PLWH who initiated treatment during chronic infection. A better understanding of the features of effector cells from PLWH who initiated ART during acute infection may provide insights into the basis of a better-preserved anti-HIV immune response and post-treatment control of HIV.

Overall, these observations suggest different ways in which HIV-infected people achieve full or partial immunological control of their infection. Understanding the basis of their success could inform strategies to eliminate infected cells or improve PLWH's ability to control HIV after ART cessation. As a step towards these goals, we undertook a deep assessment of effector T and NK cells from three categories of aviremic PLWH: elite controllers, and HIV+ ART-suppressed individuals who had started therapy either during the acute or the chronic stage of infection. We designed a 42-parameter CyTOF panel, tailored for simultaneous characterization of T and NK cells, and implemented it on freshly isolated paired blood and lymphoid tissue specimens from PLWH. By comparing across participant groups (elite controllers, acutely-treated HIV+ ART-suppressed individuals, and chronically-treated HIV+ ART-suppressed individuals), and between sampling sites (blood and LN), we define characteristics of T and NK cells that associate with a specific state of HIV control, and identify profound phenotypic differences between effector cells from blood and lymphoid tissue.

MATERIALS AND METHODS

Study Participants and Specimen Collection

The study was approved by the University of California, San Francisco (UCSF) under IRB # 10–01330, and all participants provided informed consent. Blood was drawn from 19 participants total, and for 13 participants, LN specimens were

additionally collected under local anesthesia using ultrasound-guided fine need aspiration (FNA) at the same study visit. No adverse effects from FNA procedures were reported, and participants reported minimal to no discomfort during and after the procedure. Demographical and clinical characteristics of the study's HIV+ participants are summarized in **Table S1**. Participants included: 1) 5 elite controllers, 2) 8 individuals on long-term ART who initiated therapy during acute (<1 year) infection, and 3) 6 individuals on long-term ART who initiated therapy during chronic (>1 year) infection (**Table S1**). For paired LN and blood specimens, participants included: 1) 4 elite controllers, 2) 5 individuals on long-term ART who initiated therapy during acute infection, and 3) 4 individuals on long-term ART who initiated therapy during chronic infection. All 14 individuals on ART were stably suppressed: their HIV-1 RNA load was <110 copies/ml (<40 HIV-1 RNA copies/ml in 12 participants) and their CD4 T cell count >400 cells/μL.

Isolation of Cells

PBMCs were isolated from whole-blood specimens using Lymphoprep density gradient medium according to the manufacturer's protocol (StemCell Technologies, Vancouver, BC, Canada). LN specimens were obtained by FNA biopsies of 1–2 lymph nodes in the inguinal chain area. Generally, 4–5 passes per LN were performed using 3 cc slip tip syringes and 23- or 22-gauge needles of 1 ½ inch in length. To confirm LN sample acquisition, a portion of the first pass was fixed in 95% alcohol on a slide, stained with Toluidine Blue, and examined by microscopy. Following confirmation from the cytopathologist, the remaining sample was transferred into RPMI medium (Corning, Corning, NY, USA). LN specimens were mechanically dissociated into single-cell suspension using a 5 ml syringe and a 70-micron strainer.

Preparation of Cells for CyTOF

Freshly isolated cells from blood and LN specimens were immediately treated with cisplatin (Sigma-Aldrich, St. Louis, MO, USA) as a live/dead marker and then fixed with paraformaldehyde as described previously (44–50). Briefly, a total of 6 x 10^6 cells were resuspended in 2 ml PBS (Rockland, Gilbertsville, PA, USA) with 2 mM EDTA (Corning, Corning, NY, USA). Then, 2 ml of PBS with 2 mM EDTA and 25 μM cisplatin (Sigma-Aldrich, St. Louis, MO, USA) was added to the cells, quickly mixed, and the mix incubated for 60 s at room temperature. Cisplatin staining was quenched with 10 ml CyFACS (metal contaminant-free PBS [Rockland, Gilbertsville, PA, USA] supplemented with 0.1% bovine serum albumin [BSA; Sigma-Aldrich, MO, USA] and 0.1% sodium azide [Sigma-Aldrich, St. Louis, MO, USA]). Following centrifugation, cells were resuspended in 2% paraformaldehyde (PFA, Electron Microscopy Sciences, Hatfield, PA, USA) in CyFACS and incubated for 10 min at room temperature. Cells were washed twice in CyFACS, resuspended in 100 μL of CyFACS containing 10% DMSO, and stored at −80°C until analysis by CyTOF.

CyTOF Staining and Data Acquisition

Staining of cells for CyTOF analysis was conducted as previously described (44–50). To minimize cell loss, multiple cisplatin-treated samples were barcoded and combined using the Cell-ID 20-Plex Pd Barcoding Kit (Fluidigm, South San Francisco, CA, USA), according to the manufacturer's protocol. Briefly, the fixed samples were thawed, washed twice with Maxpar Barcode Perm Buffer (Fluidigm, South San Francisco, CA, USA), and resuspended in 800 μL of Maxpar Barcode Perm Buffer in Nunc 96 DeepWell polystyrene plates (Thermo Fisher, Waltham, MA, USA). Each barcode (10 μL) was diluted in 100 μL of Maxpar Barcode Perm Buffer, added to each sample, and the mix incubated for 30 min at room temperature. Individual samples were washed once with MaxPar Cell Staining Buffer (Fluidigm, South San Francisco, CA, USA), once with CyFACS, and then combined.

Barcoded cells were aliquoted at a concentration of 6×10^6 cells/800 μL CyFACS per well into Nunc 96 DeepWell polystyrene plates. Cells were then blocked with 1.5% mouse sera (Thermo Fisher, Waltham, MA, USA), 1.5% rat sera (Thermo Fisher, Waltham, MA, USA), and 0.3% human AB sera (Sigma-Aldrich, St. Louis, MO, USA) for 15 min at 4°C. Cells were then washed twice with CyFACS and incubated for 45 min at 4°C in 100 μL/well with the cocktail of surface antibodies (**Table S2**). Cells were then washed 3X with CyFACS and incubated at 4°C overnight in 2% PFA (Electron Microscopy Services, Hatfield, PA, USA) in PBS (Rockland, Gilbertsville, PA, USA). Cells were then incubated with Intracellular Fixation and Permeabilization Buffer (eBioscience, San Diego, CA, USA) for 30 min at 4°C. Cells were then washed twice in Permeabilization Buffer (eBioscience, San Diego, USA) and blocked for 15 min at 4°C in 100 μL/well of 0.15% mouse and 0.15% rat sera diluted in Permeabilization Buffer. After washing once with Permeabilization Buffer, cells were incubated for 45 min at 4°C in 100 μl/well with the cocktail of intracellular antibodies (**Table S2**) diluted in Permeabilization Buffer. Cells were then wash once with CyFACS and incubated for 20 min at room temperature with 250 nM Cell-ID Intercalator-IR (Fluidigm, South San Francisco, CA, USA). Afterwards, cells were washed twice with CyFACS and incubated overnight at 4°C in CyFACS. Prior to sample acquisition, cells were washed once with MaxPar Cell Staining Buffer (Fluidigm, South San Francisco, CA, USA), once with Cell Acquisition Solution (Fluidigm, South San Francisco, CA, USA), and then resuspend in 1X EQ Four Element Calibration Beads (Fluidigm, South San Francisco, CA, USA) diluted in Cell Acquisition Solution (Fluidigm, South San Francisco, CA, USA). The concentration of cells was adjusted to acquire at a rate of ~300 events/sec using a wide-bore (WB) injector on a Helios-upgraded CyTOF2 instrument (Fluidigm, South San Francisco, CA, USA) at the UCSF Parnassus Flow Core Facility.

CyTOF Data Analysis

CyTOF datasets were normalized and de-barcoded according to the manufacturer's protocol (Fluidigm, South San Francisco, CA, USA), as previously validated (44–50). FlowJo software (BD Biosciences) was used to gate for events corresponding to total T cells (live, singlet, CD19-CD14-CD33-CD3+), CD4+ T cells (live, singlet, CD19-CD14-CD33-CD3+CD8-), CD8+ T cells (live, singlet, CD19-CD14-CD33-CD3+CD8+), and NK cells (CD19-CD14-CD33-CD3-CD4-CD7+) among PBMC and LN specimens (**Supplementary Figure S1**). Tissue resident memory T cells (Trm) were defined as CD45RO+CD69+ T cells. Of note, due to the lack of CD103 on our CyTOF panel, we were unable to distinguish between CD69+ Trm cells from CD69+CD103+ Trm cells. For data

visualization, tSNE analyses were performed in Cytobank software (Beckman Coulter, Brea, CA, USA) with default settings. Markers used in the upstream gating strategy and non-cellular markers (e.g., live/dead stain, Pd barcodes) were excluded as tSNE parameters. Dot plots were created using FlowJo (Ashland, OR, USA). The statistical tests used in comparison of groups are indicated within the figure legends.

For tSNE clustering of datasets comparing effector cells from the three patient groups, the Seurat R package for single-cell analysis (51) was used to define clusters of cells based on 39 CyTOF parameters, excluding CD19, CD14, and CD33, and clusters were filtered based on a minimum cell-count threshold of 50. For blood-derived T cells, 40,000 cells were down-sampled (randomly selected) to enable processing within memory limits and computational efficiency. A total of 11,338 LN NK cells, 240,804 blood NK cells, 463,722 LN T cells, and 759,966 blood T cells, were subjected to Seurat clustering. CyTOF clusters were identified using a shared nearest neighbor (SNN) graph based on the Jaccard index (52). The optimal clustering resolution parameters were determined using Random Forest (53) and a silhouette score-based assessment of clustering validity and subject-wise cross-validation. The silhouette score is a metric that assesses cluster validity based on within cluster distance and between cluster distance, and is often used to find the best number of clusters (54). The efficacy of resolution parameters ranging from 0.01 to 0.2 were tested, and silhouette scores were measured from each case. Cross-validation was used to assure the reproducibility of the optimization process. For the cross-validation, CyTOF profiles were used as input features and cluster memberships were used as labels to train a Random Forest model using N-1 subjects, where N is the total number of subjects. The rest of the data were used to predict the cells' cluster level and calculate the silhouette scores. This cross-validation procedure was performed N times, iterating through each of the subjects. Silhouette score was first averaged across cells in the same cluster and then the mean of the averaged scores was used as the final score. The optimal resolution parameter was selected based on the silhouette score trend across different resolution parameter values, using the elbow method. Finally, a generalized linear mixed model (GLMM) was used to estimate the association between cluster membership and infection status. The log odds ratio was retrieved from the coefficient estimate of each variable. To assess the association between CyTOF marker expression quantile levels and group (controller, acute-treated, chronic-treated), a linear model analysis was performed. Due to the small sample size per group, associations were not adjusted for age to maximize the statistical power to detect differences between groups. All p-values were corrected using the FDR, and a threshold of 0.05 was used to determine significance. GLMM was performed using R package lme4 (55), and linear regression was performed using the lm function in R.

RESULTS

Patient Population and Specimens

To characterize T and NK cells from aviremic PLWH, we recruited 13 HIV+ participants who donated both PBMCs and LN aspirates during the same study visit, along with an additional 6 participants who donated PBMCs alone (**Table S1**). Participants consisted of: elite controllers who were not taking ART (n=5), participants who initiated ART during acute HIV (<150 days from estimated date of infection) and were suppressed for at least 12 months at the time of sampling (acutely-treated, n=8), and participants who initiated ART during chronic HIV (>2 years from infection) and were suppressed for at least 12 months at the time of sampling (chronically-treated, n=6). Eligibility criteria for all participants were: (1) confirmed HIV-1 infection and (2) undetectable HIV-1 (<40 copies RNA/ml) for at least 12 months. For HIV+ ART-suppressed individuals, an additional eligibility criterion was 3) at least 12 months of continuous ART at study entry with no regimen changes in the preceding 24 weeks. Excluded participants were those with (1) recent hospitalization, (2) recent infection requiring systemic antibiotics, (3) recent vaccination or (4) exposure to any immunomodulatory drug (including maraviroc) in the 16 weeks prior to study, as has been previously described (56). The reason for these exclusion criteria is that these conditions might potentially alter the host immune response and/or the HIV reservoir size. Participants were consented by the investigator before any procedures took place, eligibility was confirmed, and medical history and concurrent medications ascertained. The research was approved by the University of California Committee on Human Research (CHR), and all participants provided written informed consent.

Cells were processed immediately after collection, stained with cisplatin as a viability marker, fixed with paraformaldehyde (PFA), and frozen until all donor samples were acquired. A 42-parameter CyTOF panel was established to simultaneously phenotype T and NK cells for markers of differentiation and activation states, homing receptors, and inhibitory and activating NK cell receptors (**Table S2**). Importantly, this panel enabled analysis of PFA-fixed cells that never went through cryopreservation. To avoid batch effects, all samples were barcoded, stained, and run on the mass cytometer together (Materials and Methods).

Elite Controllers and Acutely-Treated PLWH Have More Naïve T Cells in Peripheral Blood Than Chronically-Treated PLWH

We first conducted a systematic comparison of lymphocytes between the participant groups. We applied t-distributed stochastic neighbor embedding (tSNE) to qualitatively assess for overall phenotypic similarities and differences between CD4 + T cells, CD8+ T cells, and NK cells from PBMCs (**Figure 1A**) and lymph nodes (LNs; **Figure 1B**) between the 3 patient groups. Although CD4+ T cells, CD8+ T cells, and NK cells resided in distinct areas of the tSNE, these subsets occupied similar areas in the 3 participant groups. However, there were subtle differences in tSNE distribution of the T cells. In blood, there were two regions of the tSNE (**Figure 1A**, circled in black) occupied by CD8+ T cells from controllers, one of which was almost entirely absent in acutely-treated individuals, and both of which were relatively devoid in chronically-treated individuals. In LNs, one distinct region occupied by CD4+ T cells (**Figure 1B**, circled in black) in the controllers and acutely-treated individuals, was

devoid of cells in chronically-treated individuals. These results suggest some phenotypic differences in T cells between controllers, acutely-treated individuals, and chronically-treated individuals in both blood and LNs.

To investigate these differences in a more quantitative manner, we assessed the composition of the CD4+ T cell (naïve, Tn; memory, Tm; central memory, Tcm; effector memory, Tem; T follicular helper cells, Tfh; regulatory T cells, Treg), CD8+ T cell (Tn, Tm, Tcm, Tem), and NK cell subsets from PBMCs (**Figure 1C**) and LNs (**Figure 1E**), with the three main subsets of NK cells being classically defined by CD56 expression ($CD56^{bright}$, $CD56^{dim}$, CD56-) (18, 57). CD4+ and CD8+ Tn cells were significantly more frequent in the PBMCs of controllers than of chronically-treated individuals (**Figure 1C**). CD8+ Tn cells in PBMCs were also significantly more frequent in the acutely-treated than the chronically-treated group. Conversely, blood CD4+ and CD8+ Tm cells were more frequent in the chronically-treated group relative to the other two groups. As the proportion of Tn to Tm cells decreases with age (58, 59), we assessed whether the increase in Tn proportions in our controllers were accounted by younger age. In fact, our controllers were on average older than the acutely-treated participants (**Figure 1D**), suggesting that age did not account for our observations. In contrast to data from the blood, the frequencies of the analyzed CD4+, CD8+, or NK cell subsets from the LNs did not show any significant differences between the patient groups in LNs (**Figure 1E**). Together, these results indicate that in blood, controllers and acutely-treated individuals have an increased frequency of Tn cells compared to chronically-treated individuals on ART.

High-Dimensional Clustering Reveals Unique T and NK Cell Phenotypes Associated With Acutely-Treated PLWH

To take advantage of all phenotyping markers from our high-dimensional CyTOF datasets, we defined T and NK cell subsets *via* unsupervised clustering. Four clusters each of T cells and NK cells were identified from PBMCs, and six T cell and four NK cell clusters from LNs (**Figure 2A**). We then used a generalized linear mixed model (GLMM) to estimate the association between cluster membership and group. Clusters significantly associated with a specific state of HIV control were identified for blood T cells, blood NK cells, and LN T cells (**Figure 2A**). In particular, T cell Cluster 3 from blood (Acute vs. Controllers: $P < 0.0001$; Acute vs. Chronic: $P < 0.009$) and T cell Cluster 9 from LNs (Acute vs. Controllers: $P < 0.03$; Acute vs. Chronic: $P < 0.0001$) were enriched in acutely-treated individuals compared to controllers and the chronically-treated individuals. In addition, NK cell Cluster 8 from blood was enriched in acutely-treated individuals as compared to chronically-treated ones ($P < 0.05$). No significant associations with disease state were found for LN NK cells.

We then searched for unique features and expression profiles in the clusters that were over-represented among the acutely-treated group (**Figures 2B–D**; expression levels of all antigens from all clusters are shown in **Figures S2**–**S5**). Cluster 3 of blood T cells expressed relatively high levels of CD8, CD45RA, and TCF1 (**Figure 2B**), consistent with a more Tn-like phenotype (**Figure 1C**). Cluster 8 of blood NK cells preferentially expressed low levels of CD56 and included both CD16- and CD16+ cells (**Figure 2C**), the latter of which are typically rare but expanded in PLWH, and are associated with HIV control (60). Cluster 8 also expressed relatively high levels of the lymph node homing receptors CD62L and CCR7, and harbored the cells expressing the highest levels of CXCR5, suggesting these cells may be poised to migrate into the follicles of LNs. Within the LNs, Cluster 9 of T cells expressed relatively high levels of CD4, CD45RO, CD69, suggesting a T resident memory phenotype; CXCR5 and PD1, suggesting a Tfh-like phenotype; and CD127 (the alpha chain of the IL7 receptor), suggesting homeostatic proliferation potential of these cells. In sum, these data suggest acutely-treated individuals are enriched for subsets of T and NK cell exhibiting distinguishing phenotypic features.

Blood-Derived T Cells From HIV+ Individuals Are More Activated Than Those From Lymph Nodes

Having defined clusters of lymphocytes that associate with a specific state of HIV control, we next conducted comparisons between the paired PBMC and LN specimens to identify differences due to cell origin. As the overall phenotypes of T cells were overall similar between individuals (**Figures 1A, B**, **3A** *right*) we combined the data from the three patient groups together for this analysis. This analysis suggested lymphocytes from LNs to be profoundly different from their blood counterparts in that the two types of cells occupied very distinct regions of tSNE (**Figure 3A** *left*). The major subsets (Tn; Tm; Tcm; Tem; Tfh) of CD4+ (**Figure 3B**) and CD8+ (**Figure 3C**) T cells also demonstrated overall differences between blood (in grey) and LNs (in color). Manual gating also revealed different frequencies of these subsets between blood and LNs, in particular among the CD4+ Tem, CD8+ Tn, CD8+ Tm, and CD8+ Tem subsets (**Figures 3D, E**).

Interestingly, activation states differed between T cells from blood vs. LNs. When we examined the mean signal intensity (MSI) of the antigens quantitated by CyTOF (**Figures S6**, **S7**), we found the activation markers OX40, HLADR, and CD25 to be expressed at significantly higher levels on both CD4+ and CD8+ T cells from PBMCs (**Figures 3F, G**). Blood T cells also expressed higher levels of the activation marker ICOS, but this did not reach statistical significance for the CD4 subset (**Figures 3F, G**). Expression of the activation marker CD38 trended higher on blood than LN CD4+ T cells, albeit not significantly (**Figure 3F**). To confirm the elevated activation status of the blood T cells, we manually gated on T cells dually expressing CD38 and HLADR (**Figures 3H, I**), as these two markers have been used to define T cell activation state during HIV infection (61–63). CD38+HLADR+ CD4+ T cells were significantly more frequent in PBMCs than LNs (**Figure 3H**), while for CD8+ T cells, no significant differences were observed (**Figure 3I**). However, removal of one outlier individual, a controller with unusually high proportions of these cells in LNs, lead to significant differences in the CD8+ T cell compartment as well (**Figure 3I**).

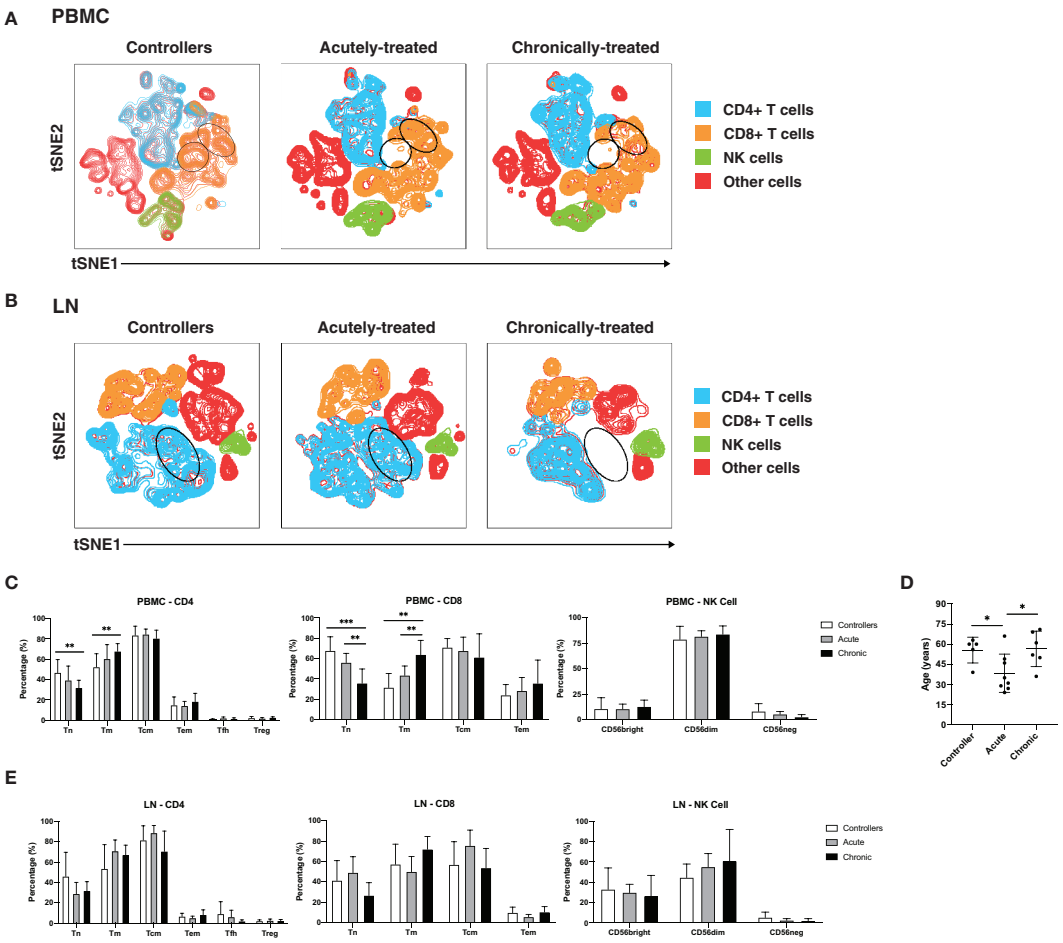

FIGURE 1 | Characterization of T and NK cells from PBMCs and LNs of HIV controllers and non-controller HIV+ individuals treated during acute or chronic infection. **(A, B)** t-distributed stochastic neighbor embedding (tSNE) plots for T and NK cells from PBMCs **(A)** and LNs **(B)** of HIV controllers (left), acutely-treated (middle), and chronically-treated (right) HIV+ individuals. The main subsets analyzed are each colored as indicated. Some subsets of T cells were preferentially detected in the controllers (regions circled in black). **(C)** Blood naïve T cells are more frequent in controllers than HIV+ ART-suppressed individuals. Shown are frequencies of canonical subsets in PBMCs from the indicated groups of HIV+ individuals among CD4+ T cells (live, singlet, CD19-CD14-CD33-CD3+CD8-, left), CD8+ T cells (live, singlet, CD19-CD14-CD33-CD3+CD8+, middle) and NK cells (CD19-CD14-CD33-CD3-CD4-CD7+, right). Subsets of CD4+ and CD8+ T cells were defined as follows: naïve T cells (Tn): CD45RO-CD45RA+; memory T cells (Tm): CD45RO+CD45RA-; central memory T cells (Tcm): CD45RO+CD45RA-CCR7+CD27+; and effector memory T cells (Tem): CD45RO+CD45RA-CCR7-CD27-. In addition, CD4+ T cells were further subsetted into T follicular helper cells (Tfh): CD45RO+CD45RA-CXCR5+PD1+; and regulatory T cells (Treg): CD45RO+CD45RA-CD25+CD127-. Subsets of NK cells were defined based on $CD56^{bright}$, $CD56^{dim}$, and CD56- staining. **(D)** Age distribution of participants in each group. Controllers were not younger than HIV+ ART-suppressed individuals. **(E)** Frequencies of canonical T and NK cell subsets from LNs are similar between controllers and HIV+ ART-suppressed individuals. Frequencies of the indicated subsets of CD4+ T cells (left), CD8+ T cells (middle), and NK cells (right) in LNs from the indicated groups are shown. *p<0.05, **p<0.01, ***p<0.001 as assessed using the Student's unpaired t test.

In contrast to the aforementioned activation markers, CD69 was increased on T cells from LNs as compared to T cells from PBMCs (**Figures 3F, G**). This is likely because while an activation marker in blood cells, CD69 is also the canonical marker for tissue resident memory T cells (Trm) (64–66). While CD103 is also commonly used alongside CD69 to identify subsets of Trm, it is not expressed on all Trm cells while CD69 appears to be more universally expressed on these cells (64, 66). Defining Trm cells as T cells, dually expressing CD45RO and CD69, we found that these cells, among both the CD4+ (**Figure 3J**) and CD8+ (**Figure 3L**) compartments, were significantly more abundant in LNs than in PBMCs. This was true even when the data was separated by the 3 patient groups (**Figures 3K, M**). Therefore, with the exception of CD69, activation markers were elevated on blood as compared to LN T cells.

Memory CD8+ T Cells Expressing CXCR5 Are Enriched in Lymph Nodes and Exhibit a Long-Lived, Inhibited Phenotype

As CXCR5 expression can direct CD8+ T cells to the follicles, a major site of HIV persistence (9, 10), we next determined to what extent CXCR5 was expressed on CD8+ Tm cells from blood and LNs. In addition to examining total Tm cells, we also examined Trm cells, the most abundant T cell subset in human tissues (67).

The percentage of Tm and Trm cells expressing CXCR5 was higher in LNs than in blood (**Figures 4A, B**). To gain a better understanding of the features of these follicular CXCR5-expressing CD8+ T cells, we compared their expression levels of homing receptors and activation/differentiation markers to that of their CXCR5- counterparts. Expression of tissue homing receptors CCR6 and CXCR4 was significantly increased on CXCR5+ cells, as was expression of the lymph node homing receptors CCR7 and CD62L (**Figure 4C**), suggesting the ability of these cells to migrate into multiple lymphoid tissues. TCF1 and CD127, associated with long-term survival of T cells, were also expressed at elevated levels on the CXCR5+ cells. As NK cell receptors have previously been reported to be expressed on T cells and to regulate their function (68), we also assessed their expression on CXCR5+ vs. CXCR5- CD8+ Tm cells (**Figure 4C**). Surprisingly, the inhibitory NK cell receptors KIR2DL1, CD94, and NKG2A were significantly increased on the CXCR5+ cells. These results suggest that within lymph nodes, CXCR5+ CD8+ T cells, relative to their CXCR5- counterparts, have broad tissue homing capabilities and are long-lived, but may be restrained in their effector functions as they express multiple markers associated with suppression of effector functions. Whether CXCR5+ NK cells exhibit similar phenotypic features could not be reliably assessed as there were too few of these cells in our specimens.

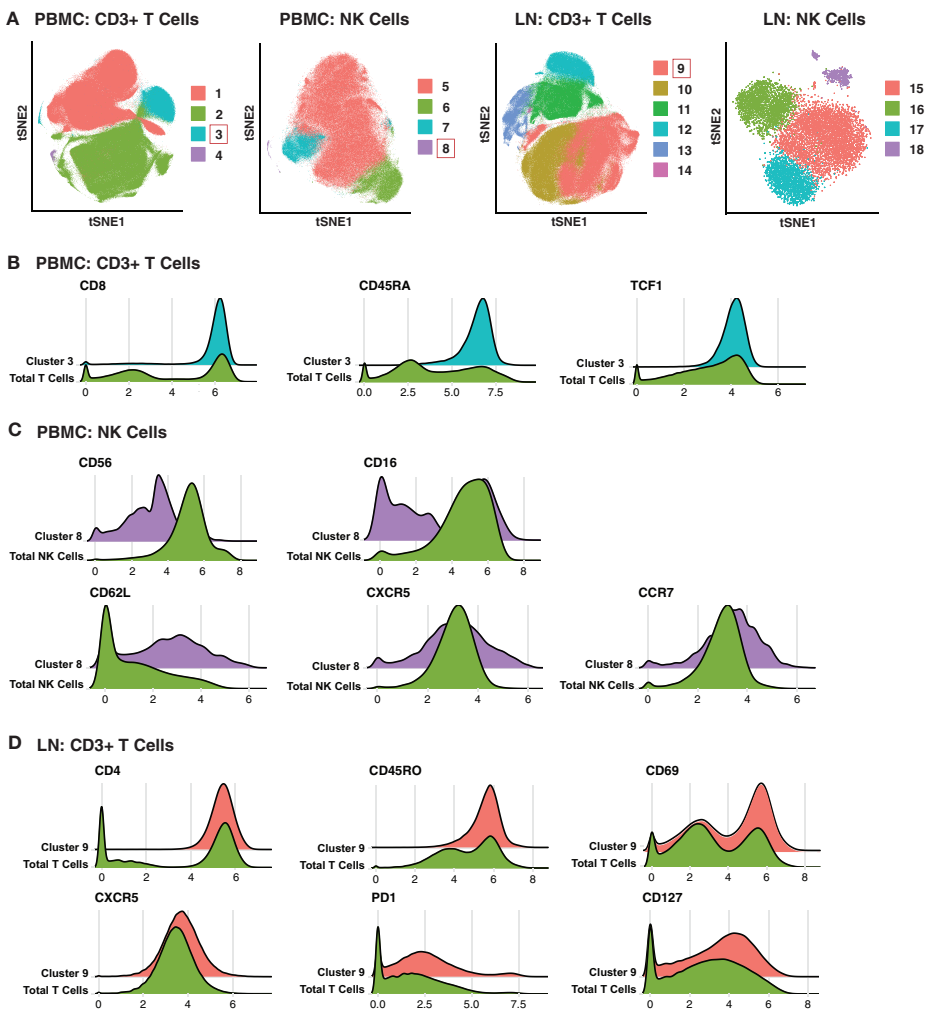

FIGURE 2 | Clusters of T and NK cells associated with acutely treatment of HIV. **(A)** tSNE visualization of T and NK cell clusters from PBMCs and LNs. Clusters significantly enriched in the acutely-treated group are boxed in red. **(B)** Cluster 3 of blood T cells was enriched in the acutely-treated group relative to controllers ($P < 0.0001$) and the chronically-treated group ($P < 0.009$). Cells in Cluster 3 expressed relatively high levels of CD8, CD45RA, CD27, CCR7, and TCF1. **(C)** Cluster 8 of blood NK cells was enriched in the acutely-treated group relative to chronically-treated group ($P < 0.05$). Cells in Cluster 8 expressed low levels of CD56, and approximately half of them were CD16+. Cluster 8 also included cells expressing high levels of lymph node-homing receptors CD62L, CCR7, and CXCR5. **(D)** Cluster 9 of LN T cells was enriched in the acutely-treated group relative to controllers ($P < 0.03$) and the chronically-treated group ($P < 0.0001$). Cluster 9 corresponded to CD4+ T cells expressing high levels of the T resident memory (Trm) marker CD69, the T follicular helper (Tfh) markers PD1 and CXCR5, and the alpha chain of the IL7 receptor CD127. A generalized linear mixed model (GLMM) was used to estimate the association between cluster membership and group (controllers, acutely-treated, or chronically-treated). The log odds ratio was retrieved from the coefficient estimate of each variable. All p-values were adjusted using the FDR, and a threshold of 0.05 was used to determine significance.

Memory-Like NK Cells Are Enriched in LNs and Express a Distinct Repertoire of Activating NK Receptors Relative to Non-Memory NK Cells

Finally, we assessed for phenotypic differences between blood- and LN-derived NK cells. NK cells from blood vs. LN were concentrated within different areas of the tSNE (**Figure 5A**), and this was true of the 3 different subsets ($CD56^{bright}$, $CD56^{dim}$, CD16-) of NK cells (**Figure 5B**). Furthermore, LNs harbored more $CD56^{bright}$ and fewer $CD56^{dim}$ NK cells than PBMCs did, but the same percentage of CD56- NK cells (**Figure 5C**).

To further assess the differences between NK cells derived from blood vs. LN, we compared the MSI for all antigens from

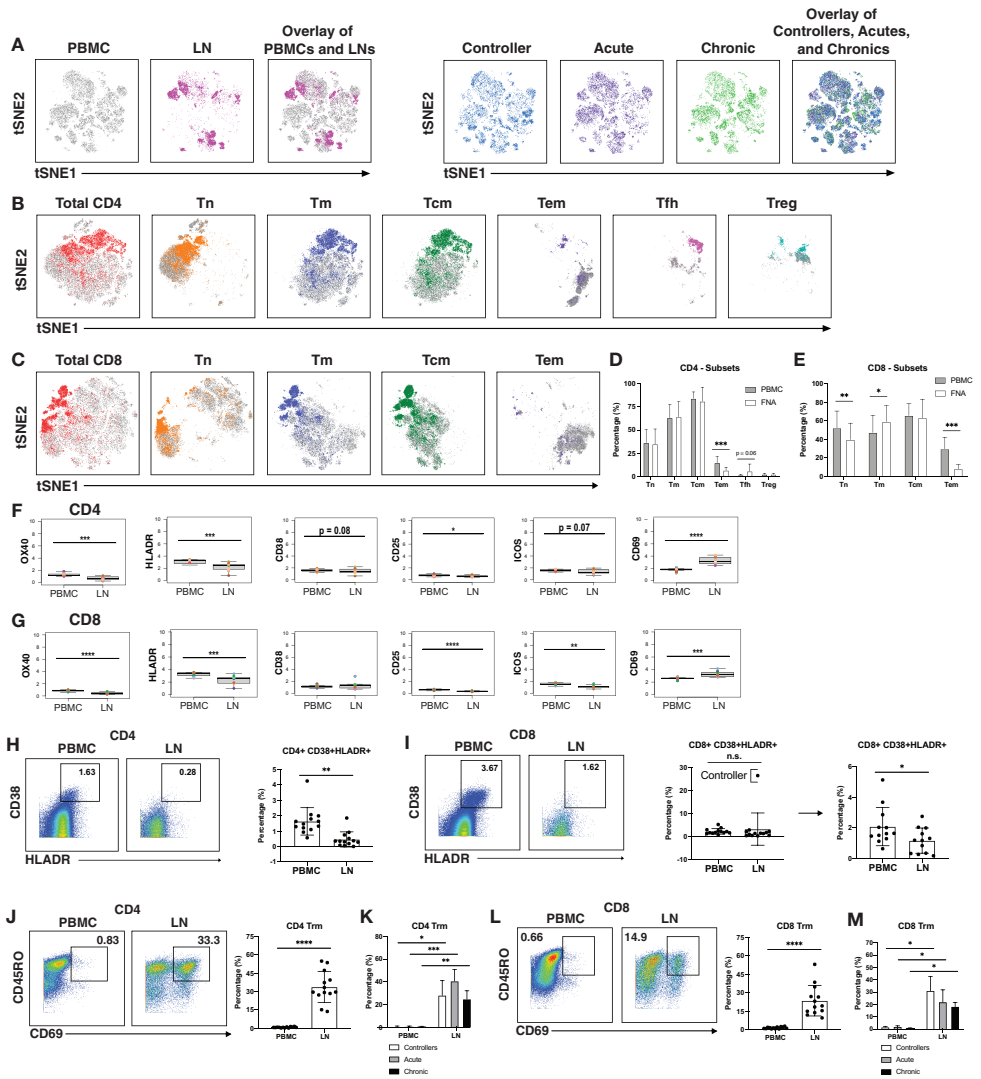

FIGURE 3 | T cells from blood of PLWH are more activated than those from lymph nodes. **(A)** tSNE plots demonstrating profound differences between T cells from blood (grey) and LNs (colored; left), and more subtle differences between patient groups (controllers in blue, acutely-treated in purple, and chronically-treated in green; right). **(B)** tSNE plots depicting phenotypic differences among subsets of CD4+ T cells from blood (grey) vs. LNs (colored). **(C)** tSNE plots depicting phenotypic differences among subsets of CD8+ T cells from blood (grey) vs. LNs (colored). CD4+ Tem **(D)** and CD8+ Tem and CD8+ Tn **(E)** are more frequent in blood than in LNs. Shown are frequencies of T cell subsets relative to total PBMC (grey bars) or LNs (white bars), displayed as bar graphs. Cell subsets are as described in the legend for **Figure 1C**. CD4+ **(F)** and CD8+ **(G)** T cells from blood express high levels of activation markers, with the exception of activation/tissue residency marker CD69. Shown are the mean signal intensity (MSI) levels of the indicated activation markers assessed in T cells from PBMCs and LNs. Data are displayed as bar graphs with individual donors' values as colored dots. The remaining antigens are presented in **Figures S6, S7**. Activated CD38+HLADR+ CD4+ **(H)** and CD8+ **(I)** T cells are more frequent in PBMCs than LNs. Gates for activation of T cells dually expressing the two activation markers CD38 and HLADR (left). The bar graphs (right) show the percentages of CD38+HLADR+ T cells in PBMCs and LNs among all donors examined. For CD8+ T cells, one extreme outlier proved to be an HIV controller; data analyzed after removing this outlier are shown on the far right. **(J , K)** CD4+ and **(L , M)** CD8+ T resident memory (Trm) cells are enriched in LNs, in all groups. Trm cells were defined as those dually expressing CD45RO and CD69 (left). Their frequencies in PBMCs and LNs are depicted as bar graphs (right). *p<0.05, **p<0.01, ***p<0.001, ****p<0.0001 as determined using the Student's paired t test and adjusted for multiple testing using the Benjamini-Hochberg for FDR.

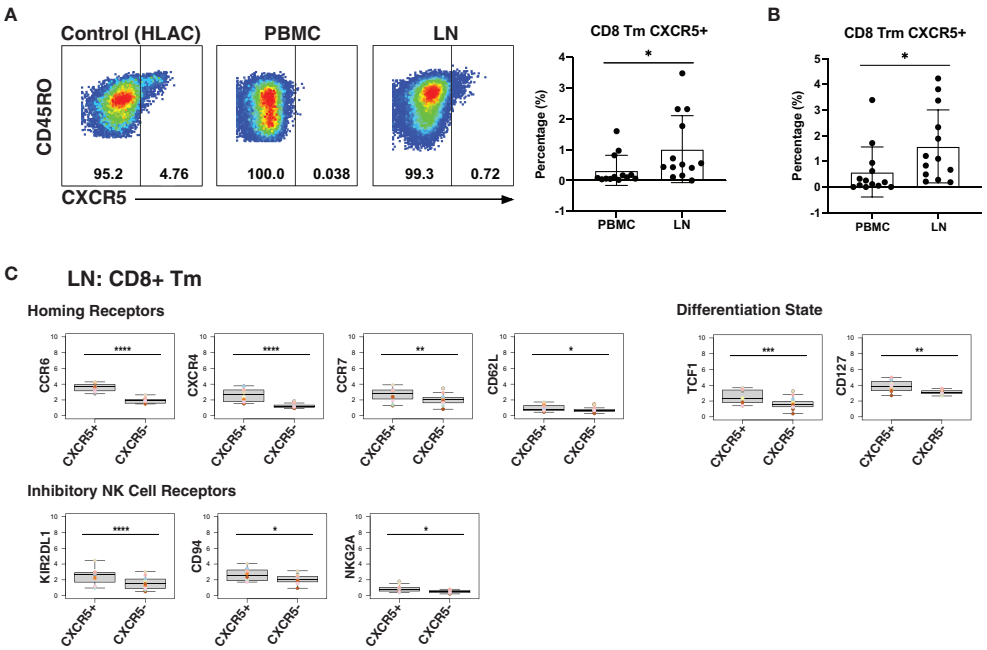

FIGURE 4 | LNs from PLWH are enriched for CXCR5+ CD8+ T cells expressing high levels of inhibitory NK cell receptors. **(A)** CXCR5+ memory T cells are more frequent in LNs than in blood. Gating strategy (left) and frequencies of CXCR5+ cells (right) among memory CD8+ T cells from paired PBMCs and LNs. The gating strategy for CXCR5+ cells was established using human lymphoid aggregate cultures (HLAC) of tonsils, which harbor a distinct population of these cells. **(B)** CXCR5+ tissue-resident memory T cells (Trm) are more frequent in LNs than in blood. **(C)** Lymphoid CXCR5+ memory CD8+ T cells express higher levels of tissue homing receptors, markers of long-lived memory cells, and inhibitory NK receptors, relative to their CXCR5- counterparts. Shown are MSIs of the indicated homing receptors, differentiation state markers, inhibitory and activating NK cell receptors. *p<0.05, **p<0.01, ***p<0.001, ****p<0.0001 as assessed using the Student's paired t test and adjusted for multiple testing using the Benjamini-Hochberg for FDR.

our CyTOF panel (**Figure S8A**). This analysis revealed that TCF1 was significantly increased in LN relative to blood NK cells (**Figure 5D**). Interestingly, *TCF7* (transcript for TCF1) marks a memory-like NK cell subset within the blood of PLWH, and this subset was hypothesized to contribute to HIV control (19). As this memory-like NK cell subset was also shown to be $CD56^{bright}$ (19), we then compared MSI expression of TCF1 between the 3 major NK cell subsets ($CD56^{bright}$, $CD56^{dim}$, CD56-). We found, as expected (19), TCF1 expression levels to be highest in the $CD56^{bright}$ subset in blood, and further demonstrated that this was true in the LN compartment as well (**Figure 5E**). Manual gating revealed that the LN harbored significantly higher proportions of these memory-like $CD56^{bright}$TCF1+ NK cells, while blood harbored more $CD56^{dim}$TCF1- NK cells (**Figure 5F**).

To better define the $CD56^{bright}$TCF1+ NK cells in LNs, we compared the MSI of markers of differentiation and activation states, homing receptors, and inhibitory and activating NK cell receptors between the $CD56^{bright}$TCF1+ (memory-like) vs. $CD56^{dim}$TCF1- (not memory-like) NK cells (**Figure 5G**). LN $CD56^{bright}$TCF1+ NK cells expressed high levels of the co-receptor CD94, an antigen recently reported to be expressed on $CD56^{bright}$TCF1+ NK cells from the blood of PLWH (19). They also expressed high levels of the LN homing receptors CCR7 and CD62L, high levels of the activation markers HLADR and ICOS, and low levels of the NK cell differentiation markers CD16 and CD57, suggesting that they may be less terminally differentiated (69). They also expressed high levels of the inhibitory receptor NKG2A, and high levels of the activation receptors NKG2D, DNAM-1, NKp46, and NKp30, relative to LN $CD56^{dim}$TCF1- NK cells. By contrast, low levels of the inhibitory receptor TIGIT were observed in these cells. Interestingly, the differences observed between $CD56^{bright}$TCF1+ and $CD56^{dim}$TCF1- NK cells from the LNs were recapitulated within the blood compartment (**Figure S8B**).

In sum, these results show that a memory-like $CD56^{bright}$ TCF1+ NK cell subset previously described in the blood of PLWH is enriched in LNs, and that these cells express high levels of multiple activation markers and activating NK cell receptors, suggesting they exist in a state of heightened activation relative to non-memory ($CD56^{dim}$TCF1-) NK cells.

DISCUSSION

In this study, we used high-parameter single-cell phenotyping by CyTOF to define the features of blood- and LN-derived T and NK cells from three groups of aviremic PLWH: elite controllers, and HIV+ ART-suppressed individuals who had initiated ART during the acute vs. chronic phases of infection. Our main

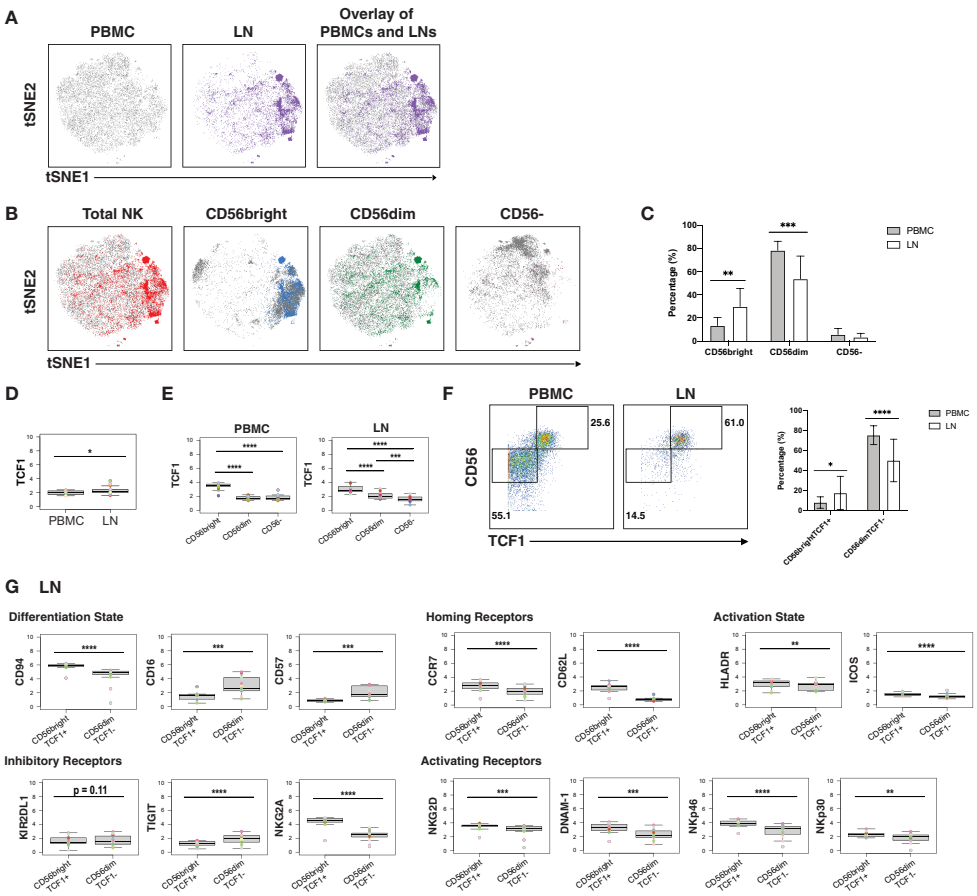

FIGURE 5 | CD56^{bright} NK cells from PLWH display phenotypic features of memory and are enriched in LNs. **(A)** tSNE plots demonstrating the overall differences between total NK cells from blood (grey) and LN (colored). **(B)** NK cell subsets, defined by CD56 expression (total, CD56^{bright}, CD56^{dim}, CD56-), are phenotypically distinct in blood (grey) as compared to LNs (colored). **(C)** NK cells from PBMCs have increased frequencies of CD56^{dim} cells, while NK cells from LNs have increased frequencies of CD56^{bright} cells. Shown are the percentages of the indicated populations among total NK cells. **(D)** TCF1 expression is higher in NK cells from LNs than from blood. MSI of TCF1 in total NK cells from PBMCs and LNs are shown. Expression levels of other antigens on these two cell populations are presented in **Figure S8**. **(E)** TCF1 expression is highest in the CD56^{bright} subset of NK cells. MSI of TCF1 in NK cell subsets from PBMCs and LNs are shown. **(F)** LNs harbor a larger proportion of CD56^{bright}TCF1+ NK cells than do PBMCs. Representative gates (left) and frequencies (right) of CD56^{bright}TCF1+ and CD56^{dim}TCF1- NK cells in PBMCs and LNs. **(G)** LN CD56^{bright}TCF1+ NK cells are less differentiated and express increased levels of LN homing receptors, activation markers, and activating NK receptors than LN CD56^{dim}TCF1- NK cells. Shown are MSI levels of the indicated markers assessed in CD56^{bright}TCF1+ and CD56^{dim}TCF1- NK cells from LNs. Plots comparing MSI of the indicated markers between CD56^{bright}TCF1+ and CD56^{dim}TCF1- NK cells from PBMCs are presented in **Figure S8**. *p<0.05, **p<0.01, ***p<0.001, ****p<0.0001 as assessed using the Student's paired t test and for MSIs, adjusted for multiple testing using the Benjamini-Hochberg for FDR.

findings are that T and NK cells from the acutely-treated individuals harbour unique phenotypic features, and differ markedly depending on whether they derived from the blood or LN compartment.

Three clusters of cells were significantly enriched in the acutely-treated individuals. One of these (Cluster 3) corresponded to Tn cells. The second, Cluster 8, corresponded to NK cells that express high levels of the homing receptors CD62L, CCR7, and CXCR5, suggesting the ability of these cells to migrate into or be retained within the LN follicle. Interestingly, Cluster 8 included the CD56-CD16+ subset of NK cells enriched within HIV+ individuals who produce broadly neutralizing antibodies (bnAbs) against HIV (60), suggesting these NK cells may facilitate bnAb production to control HIV replication. How these NK cells may do this is unclear, but may relate to the fact that, unlike CD56+ NK cells, they are unable to restrict the stimulation of antibody production by CD4+ T cells (60), and therefore may better a T-dependent antibody response. Consistent with this hypothesis, Cluster 9, which like Cluster 8 was over-represented in the acutely-treated group, consisted of LN CD4+ T cells that exhibited features of Tfh, which are known to be important for providing help to B cells, and that expressed high levels of CD127, which promotes T cell survival and proliferation (70, 71). Because individuals who initiated ART during the acute phase of infection are more likely to become post-treatment controllers (PTCs) upon treatment

interruption (ATI) (32, 34–36), future studies should determine if CD56-CD16+ NK cells and CD127-expressing Tfh-like CD4+ T cells are enriched in PTCs, as this would suggest these cells may be involved in viremic control after ART withdrawal.

In-depth comparisons of CD8+ T cells from the blood and tissue compartments from our cohort revealed that those from LNs were relatively quiescent, and preferentially expressed CXCR5. As CXCR5+ CD8+ T cells are poised to enter the LN follicle where much of the HIV reservoir resides (3–6), they have the potential to control viral replication. However, we found that these cells expressed elevated levels of a number of inhibitory NK cell receptors, including KIR2DL1, NKG2A, and NKG2A's co-receptor CD94, which can dampen CD8+ T cells' effector function (72–74). Our finding that expression of these receptors is elevated on LN CD8+ T cells, suggests that within the lymphoid compartment these cells may be preferentially restricted in their effector functions. This lack of effector CD8+ T cell function within the LNs could possibly be acting as a regulatory mechanism to avoid damaging host tissues. Similarly, T cell exhaustion, common during HIV infection, may further help prevent excessive tissue damage. Consistent with this notion are recent reports that LN HIV-specific CXCR5+ CD8+ T cells from both controller and non-controller PLWH exhibit poor cytolytic activity *ex vivo* (13, 14). Therefore, strategies aimed to eradicate the lymphoid tissue HIV reservoir may need to not only increase CD8+ T cell entry into the B cell follicle, but also release the intrinsic breaks on their cytolytic or other effector mechanisms, perhaps through antagonism of these inhibitory receptors.

There was also an enrichment of a unique subset of memory-like NK cells in LNs of PLWH. These cells, identified as $CD56^{bright}$TCF1+ NK cells, are phenotypically similar to memory-like NK cells previously described in the blood of PLWH (19). In both the blood and LN compartments, the $CD56^{bright}$TCF1+ NK cells exhibited decreased expression of NK cell maturation markers CD16 and CD57, and increased expression of the homing receptors CCR7 and CD62L, relative to their $CD56^{dim}$TCF1- counterparts. They also expressed increased levels of the activation markers HLADR and ICOS, increased expression of the NKG2A/C co-receptor CD94, and activating receptors NKG2D, DNAM1, NKp46, and NKp30. These results suggest overall phenotypic similarities between these memory-like NK cells in the blood and LN compartments. Interestingly, memory-like $CD56^{bright}$ NK cells were recently described in BLT humanized mice vaccinated with HIV envelope protein, and these cells, like the ones we have characterized, also expressed decreased levels of CD16 and CD57, and increased levels of CD62L and NKG2A (17). As these BLT tissue-derived memory-like NK cells were capable of mediating antigen-specific recall responses *ex vivo* (17), the LN $CD56^{bright}$TCF1+ NK we characterized may also be capable of mediating such recall responses. These LN $CD56^{bright}$TCF1+ NK cells may play an active role in controlling HIV replication within tissues, although future studies will be required to directly test this. In summary, memory-like $CD56^{bright}$TCF1+ NK cells are enriched in the lymphoid compartment and exhibit similar phenotypic features as their blood counterparts, including expression of numerous NK activating receptors which may aid in their ability to respond to and kill HIV-infected cells.

Our study has limitations. Our sample size was small and the findings reported here should be validated in larger cohorts. Additionally, due to the limited number of cells available (particularly from LNs), we were unable to evaluate functional responses of T and NK cells. Future studies should define how the blood and lymphoid T and NK cell subsets characterized here respond to HIV-infected target cells and how these cells compare to those in HIV-uninfected individuals. Further, this study was not set up to collect serum at the time of sample acquisition, so we were unable to analyze the association of inflammatory markers with our T and NK cell phenotyping data. Despite these limitations, our data strongly suggest that the phenotypic features of T and NK cells are affected by the timing of when ART is initiated during HIV infection, and whether these cells are isolated from the blood or LNs. We find that CXCR5-expressing CD8+ T cells and memory-like NK cells are both enriched within the LNs of PLWH. These effector cells may be good candidates to unleash for immune-based therapeutic approaches to achieve ART-free HIV remission.

DATA AVAILABILITY STATEMENT

The raw datasets generated for this study can be found in the public repository Dryad, and accessible at the following link: https://doi.org/10.7272/Q6CV4FZJ.

ETHICS STATEMENT

The studies involving human participants were reviewed and approved by University of California Committee on Human Research (CHR). The patients/participants provided their written informed consent to participate in this study.

AUTHOR CONTRIBUTIONS

AFG designed and conducted experiments, conducted data analysis, and wrote the manuscript. XL wrote scripts for data analysis. JN provided technical advice. SGD established the SCOPE cohort. RH conducted SCOPE participant enrollment. SGD and SAL established the UCSF Acute HIV study within the SCOPE cohort. SAL conducted the acute HIV participant enrollment, and PV conducted specimen collection. M-GS and RT provided bioinformatics assistance. CAB provided technical advice. WCG supervised data analysis and edited the manuscript. SAL and NRR conceived ideas and SGD, WG, SAL, and NRR obtained funding to support the study. NRR designed experiments, edited the manuscript, and supervised the study. All authors read and approved the manuscript.

FUNDING

This work was supported by the following grants: National Institutes of Health R01 AI147777 (NRR); National Institutes of Health P01 AI131374 (WCG); amfAR Institute for HIV Cure Research 109380-59-RGRL (SGD, SAL, NRR); Gilead Sciences Investigator-Initiated Grant IN-US-236-1354 (SAL); Viiv Health Investigator-Initiated Grant CA-0101618 (SAL), UM1 AI164559 and UM1 AI164567 (NRR).

ACKNOWLEDGMENTS

We acknowledge NIH DRC Center grant P30 DK063720 and S10 1S10OD018040-01 for use of the CyTOF instrument. We also thank S Tamaki, TK Peech, and C Bispo for CyTOF assistance at the Parnassus Flow Core; V Tai and M Kerbleski for assistance with the SCOPE specimens; F Chanut for editorial assistance; and R Givens for administrative assistance. Gladstone Institutes thanks the James B. Pendleton Charitable Trust for generous funding of equipment in support of HIV research.

SUPPLEMENTARY MATERIAL

The Supplementary Material for this article can be found online at: https://www.frontiersin.org/articles/10.3389/fimmu.2022.803417/full#supplementary-material

Supplementary Figures 1 | CyTOF gating strategy to identify total T cells, CD4+ T cells, CD8+ T cells, and NK cells from PBMCs and LNs of PLWH. **(A)** Shown are gating strategies to identify live, singlet, total T cells, CD4+ T cells, and CD8+ T cells from a representative PBMC and LN specimen. **(B)** Shown are gating strategies to identify live, singlet NK cells from a representative PBMC and LN specimen.

Supplementary Figures 2 | Expression levels of antigens on Seurat-identified clusters of T cells from PBMCs of PLWH. Shown are histogram plots depicting expression levels of the indicated antigens on PBMC T cells (live, singlet, CD19-CD14-CD33-CD3+) cells from clusters identified in . For a detailed explanation on how the datasets were clustered, see *Materials and Methods*.

Supplementary Figures 3 | Expression levels of antigens on Seurat-identified clusters of NK cells from PBMCs of PLWH. Expression levels of the indicated antigens on PBMC NK cells (CD19-CD14-CD33-CD3-CD4-CD7+) from clusters identified in are depicted as histogram plots.

Supplementary Figures 4 | Expression levels of antigens on Seurat-identified clusters of T cells from LNs. Expression levels of the indicated antigens on LN T cells (live, singlet, CD19-CD14-CD33-CD3+) from clusters identified in are depicted as histogram plots.

Supplementary Figures 5 | Expression levels of antigens on Seurat-identified clusters of NK cells from LNs. Expression levels of the indicated antigens on LN NK cells (CD19-CD14-CD33-CD3-CD4-CD7+) from clusters identified in are depicted as histogram plots.

Supplementary Figures 6 | Expression levels of 39 surface and intracellular antigens in CD4+ T cells from PBMCs and LNs of PLWH. Shown are the mean signal intensity (MSI) values of CD4+ T cells from PBMCs as compared to LNs. *p<0.05, **p<0.01, ***p<0.001, ****p<0.0001 as assessed using the Student's unpaired t-test and adjusted for multiple testing using the Benjamini-Hochberg for FDR.

Supplementary Figures 7 | Expression levels of 39 surface and intracellular antigens in CD8+ T cells from PBMCs and LNs of PLWH. Shown are the mean signal intensity (MSI) values of CD8+ T cells from PBMCs as compared to LNs. *p<0.05, **p<0.01, ***p<0.001, ****p<0.0001 as assessed using the Student's unpaired t-test and adjusted for multiple testing using the Benjamini-Hochberg for FDR.

Supplementary Figures 8 | Expression levels of 39 surface and intracellular antigens in NK cells from PBMCs and LNs of PLWH. **(A, B)** Mean signal intensity (MSI) values comparing NK cells from PBMCs vs. LNs **(A)**, or between $CD56^{bright}$TCF1+ and $CD56^{dim}$TCF1- NK cells from PBMCs **(B)**. PBMC $CD56^{bright}$TCF1+ cells are less differentiated and express higher levels of LN homing receptors, activation markers, and activating NK receptors than do PBMC $CD56^{dim}$TCF1- NK cells. *p<0.05, **p<0.01, ***p<0.001, ****p<0.0001 as determined using the Student's unpaired t-test and adjusted for multiple testing using the Benjamini-Hochberg for FDR.

REFERENCES

1. Bjorkstrom NK, Strunz B, Ljunggren HG. Natural Killer Cells in Antiviral Immunity. *Nat Rev Immunol* (2021) doi. doi: 10.1038/s41577-021-00558-3
2. Estes JD, Kityo C, Ssali F, Swainson L, Makamdop KN, Del Prete GQ, et al. Defining Total-Body AIDS-Virus Burden With Implications for Curative Strategies. *Nat Med* (2017) 23(11):1271–6. doi: 10.1038/nm.4411
3. Brenchley JM, Vinton C, Tabb B, Hao XP, Connick E, Paiardini M, et al. Differential Infection Patterns of CD4+ T Cells and Lymphoid Tissue Viral Burden Distinguish Progressive and Nonprogressive Lentiviral Infections. *Blood* (2012) 120(20):4172–81. doi: 10.1182/blood-2012-06-437608
4. Lindqvist M, van Lunzen J, Soghoian DZ, Kuhl BD, Ranasinghe S, Kranias G, et al. Expansion of HIV-Specific T Follicular Helper Cells in Chronic HIV Infection. *J Clin Invest* (2012) 122(9):3271–80. doi: 10.1172/JCI64314
5. Perreau M, Savoye AL, De Crignis E, Corpataux JM, Cubas R, Haddad EK, et al. Follicular Helper T Cells Serve as the Major CD4 T Cell Compartment for HIV-1 Infection, Replication, and Production. *J Exp Med* (2013) 210 (1):143–56. doi: 10.1084/jem.20121932
6. Banga R, Procopio FA, Noto A, Pollakis G, Cavassini M, Ohmiti K, et al. PD-1+ and Follicular Helper T Cells Are Responsible for Persistent HIV-1 Transcription in Treated Aviremic Individuals. *Nat Med* (2016) 22:754–61. doi: 10.1038/nm.4113
7. Carrega P, Ferlazzo G. Natural Killer Cell Distribution and Trafficking in Human Tissues. *Front Immunol* (2012) 3:347. doi: 10.3389/fimmu.2012.00347
8. Leong YA, Chen Y, Ong HS, Wu D, Man K, Deleage C, et al. CXCR5(+) Follicular Cytotoxic T Cells Control Viral Infection in B Cell Follicles. *Nat Immunol* (2016) 17(10):1187–96. doi: 10.1038/ni.3543
9. Ayala VI, Deleage C, Trivett MT, Jain S, Coren LV, Breed MW, et al. CXCR5-Dependent Entry of CD8 T Cells Into Rhesus Macaque B-Cell Follicles Achieved Through T-Cell Engineering. *J Virol* (2017) 91(11):1–17. doi: 10.1128/JVI.02507-16
10. Haran KP, Hajduczki A, Pampusch MS, Mwakalundwa G, Vargas-Inchaustegui DA, Rakasz EG, et al. Simian Immunodeficiency Virus (SIV)-Specific Chimeric Antigen Receptor-T Cells Engineered to Target B Cell Follicles and Suppress SIV Replication. *Front Immunol* (2018) 9:492. doi: 10.3389/fimmu.2018.00492
11. Watson DC, Moysi E, Valentin A, Bergamaschi C, Devasundaram S, Fortis SP, et al. Treatment With Native Heterodimeric IL-15 Increases Cytotoxic Lymphocytes and Reduces SHIV RNA in Lymph Nodes. *PloS Pathog* (2018) 14(2):e1006902. doi: 10.1371/journal.ppat.1006902
12. Webb GM, Li S, Mwakalundwa G, Folkvord JM, Greene JM, Reed JS, et al. The Human IL-15 Superagonist ALT-803 Directs SIV-Specific CD8(+) T Cells Into B-Cell Follicles. *Blood Adv* (2018) 2(2):76–84. doi: 10.1182/bloodadvances.2017012971
13. Reuter MA, Del Rio Estrada PM, Buggert M, Petrovas C, Ferrando-Martinez S, Nguyen S, et al. HIV-Specific CD8(+) T Cells Exhibit Reduced and Differentially Regulated Cytolytic Activity in Lymphoid Tissue. *Cell Rep* (2017) 21(12):3458–70. doi: 10.1016/j.celrep.2017.11.075

14. Nguyen S, Deleage C, Darko S, Ransier A, Truong DP, Agarwal D, et al. Elite Control of HIV is Associated With Distinct Functional and Transcriptional Signatures in Lymphoid Tissue CD8(+) T Cells. *Sci Transl Med* (2019) 11 (523):1–12. doi: 10.1126/scitranslmed.aax4077
15. Huot N, Jacquelin B, Garcia-Tellez T, Rascle P, Ploquin MJ, Madec Y, et al. Natural Killer Cells Migrate Into and Control Simian Immunodeficiency Virus Replication in Lymph Node Follicles in African Green Monkeys. *Nat Med* (2017) 23(11):1277–86. doi: 10.1038/nm.4421
16. Peppa D, Pedroza-Pacheco I, Pellegrino P, Williams I, Maini MK, Borrow P. Adaptive Reconfiguration of Natural Killer Cells in HIV-1 Infection. *Front Immunol* (2018) 9:474. doi: 10.3389/fimmu.2018.00474
17. Nikzad R, Angelo LS, Aviles-Padilla K, Le DT, Singh VK, Bimler L, et al. Human Natural Killer Cells Mediate Adaptive Immunity to Viral Antigens. *Sci Immunol* (2019) 4(35):1–13. doi: 10.1126/sciimmunol.aat8116
18. Vendrame E, Seiler C, Ranganath T, Zhao NQ, Vergara R, Alary M, et al. TIGIT is Upregulated by HIV-1 Infection and Marks a Highly Functional Adaptive and Mature Subset of Natural Killer Cells. *AIDS* (2020) 34(6):801–13. doi: 10.1097/QAD.0000000000002488
19. Wang Y, Lifshitz L, Gellatly K, Vinton CL, Busman-Sahay K, McCauley S, et al. HIV-1-Induced Cytokines Deplete Homeostatic Innate Lymphoid Cells and Expand TCF7-Dependent Memory NK Cells. *Nat Immunol* (2020) 21 (3):274–86. doi: 10.1038/s41590-020-0593-9
20. Kuo CT, Leiden JM. Transcriptional Regulation of T Lymphocyte Development and Function. *Annu Rev Immunol* (1999) 17:149–87. doi: 10.1146/annurev.immunol.17.1.149
21. Zhou X, Yu S, Zhao DM, Harty JT, Badovinac VP, Xue HH. Differentiation and Persistence of Memory CD8(+) T Cells Depend on T Cell Factor 1. *Immunity* (2010) 33(2):229–40. doi: 10.1016/j.immuni.2010.08.002
22. Hu PF, Hultin LE, Hultin P, Hausner MA, Hirji K, Jewett A, et al. Natural Killer Cell Immunodeficiency in HIV Disease is Manifest by Profoundly Decreased Numbers of CD16+CD56+ Cells and Expansion of a Population of CD16dimCD56- Cells With Low Lytic Activity. *J Acquir Immune Defic Syndr Hum Retrovirol* (1995) 10(3):331–40. doi: 10.1097/00042560-199511000-00005
23. Betts MR, Nason MC, West SM, De Rosa SC, Migueles SA, Abraham J, et al. HIV Nonprogressors Preferentially Maintain Highly Functional HIV-Specific CD8+ T Cells. *Blood* (2006) 107(12):4781–9. doi: 10.1182/blood-2005-12-4818
24. Korencak M, Byrne M, Richter E, Schultz BT, Juszczak P, Ake JA, et al. Effect of HIV Infection and Antiretroviral Therapy on Immune Cellular Functions. *JCI Insight* (2019) 4(12):1–14. doi: 10.1172/jci.insight.126675
25. Nabatanzi R, Bayigga L, Cose S, Rowland-Jones S, Canderan G, Joloba M, et al. Aberrant Natural Killer (NK) Cell Activation and Dysfunction Among ART-Treated HIV-Infected Adults in an African Cohort. *Clin Immunol* (2019) 201:55–60. doi: 10.1016/j.clim.2019.02.010
26. Migueles SA, Osborne CM, Royce C, Compton AA, Joshi RP, Weeks KA, et al. Lytic Granule Loading of CD8+ T Cells is Required for HIV-Infected Cell Elimination Associated With Immune Control. *Immunity* (2008) 29(6):1009–21. doi: 10.1016/j.immuni.2008.10.010
27. International H.I.V.C.S., Pereyra F, Jia X, McLaren PJ, Telenti A, de Bakker PI, et al. The Major Genetic Determinants of HIV-1 Control Affect HLA Class I Peptide Presentation. *Science* (2010) 330(6010):1551–7. doi: 10.1126/science.1195271
28. Avettand-Fenoel V, Bayan T, Gardiennet E, Boufassa F, Lopez P, Lecuroux C, et al. Dynamics in HIV-DNA Levels Over Time in HIV Controllers. *J Int AIDS Soc* (2019) 22(1):e25221. doi: 10.1002/jia2.25221
29. Gaiha GD, Rossin EJ, Urbach J, Landeros C, Collins DR, Nwonu C, et al. Structural Topology Defines Protective CD8(+) T Cell Epitopes in the HIV Proteome. *Science* (2019) 364(6439):480–4. doi: 10.1126/science.aav5095
30. Monel B, McKeon A, Lamothe-Molina P, Jani P, Boucau J, Pacheco Y, et al. HIV Controllers Exhibit Effective CD8(+) T Cell Recognition of HIV-1-Infected Non-Activated CD4(+) T Cells. *Cell Rep* (2019) 27142-153(1):e144. doi: 10.1016/j.celrep.2019.03.016
31. Casado C, Galvez C, Pernas M, Tarancon-Diez L, Rodriguez C, Sanchez-Merino V, et al. Permanent Control of HIV-1 Pathogenesis in Exceptional Elite Controllers: A Model of Spontaneous Cure. *Sci Rep* (2020) 10(1):1902. doi: 10.1038/s41598-020-58696-y
32. Saez-Cirion A, Bacchus C, Hocqueloux L, Avettand-Fenoel V, Girault I, Lecuroux C, et al. Post-Treatment HIV-1 Controllers With a Long-Term Virological Remission After the Interruption of Early Initiated Antiretroviral Therapy ANRS VISCONTI Study. *PloS Pathog* (2013) 9(3):e1003211. doi: 10.1371/journal.ppat.1003211
33. Scott-Algara D, Didier C, Arnold V, Cummings J-S, Boufassa F, Lambotte O, et al. Post-Treatment Controllers Have Particular NK Cells With High Anti-HIV Capacity: VISCONTI Study. In: *Conference on Retroviruses and Opportunistic Infections*. Seattle, Washington (2015).
34. Lodi S, Meyer L, Kelleher AD, Rosinska M, Ghosn J, Sannes M, et al. Immunovirologic Control 24 Months After Interruption of Antiretroviral Therapy Initiated Close to HIV Seroconversion. *Arch Intern Med* (2012) 172 (16):1252–5. doi: 10.1001/archinternmed.2012.2719
35. Maenza J, Tapia K, Holte S, Stekler JD, Stevens CE, Mullins JI, et al. How Often Does Treatment of Primary HIV Lead to Post-Treatment Control? *Antivir Ther* (2015) 20(8):855–63. doi: 10.3851/IMP2963
36. Sneller MC, Justement JS, Gittens KR, Petrone ME, Clarridge KE, Proschan MA, et al. A Randomized Controlled Safety/Efficacy Trial of Therapeutic Vaccination in HIV-Infected Individuals Who Initiated Antiretroviral Therapy Early in Infection. *Sci Transl Med* (2017) 9(419):1–10. doi: 10.1126/scitranslmed.aan8848
37. Jain V, Hartogensis W, Bacchetti P, Hunt PW, Hatano H, Sinclair E, et al. Antiretroviral Therapy Initiated Within 6 Months of HIV Infection is Associated With Lower T-Cell Activation and Smaller HIV Reservoir Size. *J Infect Dis* (2013) 208(8):1202–11. doi: 10.1093/infdis/jit311
38. Chun TW, Justement JS, Moir S, Hallahan CW, Maenza J, Mullins JI, et al. Decay of the HIV Reservoir in Patients Receiving Antiretroviral Therapy for Extended Periods: Implications for Eradication of Virus. *J Infect Dis* (2007) 195(12):1762–4. doi: 10.1086/518250
39. Hocqueloux L, Avettand-Fenoel V, Jacquot S, Prazuck T, Legac E, Melard A, et al. Long-Term Antiretroviral Therapy Initiated During Primary HIV-1 Infection is Key to Achieving Both Low HIV Reservoirs and Normal T Cell Counts. *J Antimicrob Chemother* (2013) 68(5):1169–78. doi: 10.1093/jac/dks533
40. Takata H, Buranapraditkun S, Kessing C, Fletcher JL, Muir R, Tardif V, et al. Delayed Differentiation of Potent Effector CD8(+) T Cells Reducing Viremia and Reservoir Seeding in Acute HIV Infection. *Sci Transl Med* (2017) 9 (377):1–9. doi: 10.1126/scitranslmed.aag1809
41. Ndhlovu ZM, Kazer SW, Nkosi T, Ogunshola F, Muema DM, Anmole G, et al. Augmentation of HIV-Specific T Cell Function by Immediate Treatment of Hyperacute HIV-1 Infection. *Sci Transl Med* (2019) 11(493):1–15. doi: 10.1126/scitranslmed.aau0528
42. Kazer SW, Walker BD, Shalek AK. Evolution and Diversity of Immune Responses During Acute HIV Infection. *Immunity* (2020) 53(5):908–24. doi: 10.1016/j.immuni.2020.10.015
43. Leyre L, Kroon E, Vandergeeten C, Sacdalan C, Colby DJ, Buranapraditkun S, et al. Abundant HIV-Infected Cells in Blood and Tissues Are Rapidly Cleared Upon ART Initiation During Acute HIV Infection. *Sci Transl Med* (2020) 12 (533). doi: 10.1126/scitranslmed.aav3491
44. Cavrois M, Banerjee T, Mukherjee G, Raman N, Hussien R, Rodriguez BA, et al. Mass Cytometric Analysis of HIV Entry, Replication, and Remodeling in Tissue CD4+ T Cells. *Cell Rep* (2017) 20(4):984–98. doi: 10.1016/j.celrep.2017.06.087
45. Ma T, Luo X, George AF, Mukherjee G, Sen N, Spitzer TL, et al. HIV Efficiently Infects T Cells From the Endometrium and Remodels Them to Promote Systemic Viral Spread. *Elife* (2020) 9:e55487. doi: 10.7554/eLife.55487
46. Neidleman J, Luo X, Frouard J, Xie G, Gill G, Stein ES, et al. SARS-Cov-2-Specific T Cells Exhibit Phenotypic Features of Helper Function, Lack of Terminal Differentiation, and High Proliferation Potential. *Cell Rep Med* (2020) 1(6):100081. doi: 10.1016/j.xcrm.2020.100081
47. Neidleman J, Luo X, Frouard J, Xie G, Hsiao F, Ma T, et al. Phenotypic Analysis of the Unstimulated In Vivo HIV CD4 T Cell Reservoir. *Elife* (2020) 9:e55487. doi: 10.7554/eLife.60933
48. Ma T, Ryu H, McGregor M, Babcock B, Neidleman J, Xie G, et al. Protracted Yet Coordinated Differentiation of Long-Lived SARS-Cov-2-Specific CD8(+) T Cells During Convalescence. *J Immunol* (2021) 207(5):1344–56. doi: 10.4049/jimmunol.2100465
49. Neidleman J, Luo X, George AF, McGregor M, Yang J, Yun C, et al. Distinctive Features of SARS-Cov-2-Specific T Cells Predict Recovery From Severe COVID-19. *Cell Rep* (2021) 36(3):109414. doi: 10.1016/j.celrep.2021.109414

50. Xie G, Luo X, Ma T, Frouard J, Neidleman J, Hoh R, et al. Characterization of HIV-Induced Remodeling Reveals Differences in Infection Susceptibility of Memory CD4(+) T Cell Subsets. *vivo Cell Rep* (2021) 35(4):109038. doi: 10.1016/j.celrep.2021.109038
51. Satija R, Farrell JA, Gennert D, Schier AF, Regev A. Spatial Reconstruction of Single-Cell Gene Expression Data. *Nat Biotechnol* (2015) 33(5):495–502. doi: 10.1038/nbt.3192
52. Levine JH, Simonds EF, Bendall SC, Davis KL, Amir el AD, Tadmor MD, et al. Data-Driven Phenotypic Dissection of AML Reveals Progenitor-Like Cells That Correlate With Prognosis. *Cell* (2015) 162(1):184–97. doi: 10.1016/j.cell.2015.05.047
53. Shin MG, Bulyntsev SV, Chang PL, Korbu LB, Carrasquila-Garcia N, Vishnyakova MA, et al. Multi-Trait Analysis of Domestication Genes in Cicer Arietinum - Cicer Reticulatum Hybrids With a Multidimensional Approach: Modeling Wide Crosses for Crop Improvement. *Plant Sci* (2019) 285:122–31. doi: 10.1016/j.plantsci.2019.04.018
54. Lovmar L, Ahlford A, Jonsson M, Syvanen AC. Silhouette Scores for Assessment of SNP Genotype Clusters. *BMC Genomics* (2005) 6:35. doi: 10.1186/1471-2164-6-35
55. Bates D, Machler M, Bolker BM, Walker SC. Fitting Linear Mixed-Effects Models Using Lme4. *J Stat Software* (2015) 67(1):1–48. doi: 10.18637/jss.v067.i01
56. Lee SA, Bacchetti P, Chomont N, Fromentin R, Lewin SR, O'Doherty U, et al. Anti-HIV Antibody Responses and the HIV Reservoir Size During Antiretroviral Therapy. *PloS One* (2016) 11(8):e0160192. doi: 10.1371/journal.pone.0160192
57. Zhao NQ, Vendrame E, Ferreira AM, Seiler C, Ranganath T, Alary M, et al. Natural Killer Cell Phenotype is Altered in HIV-Exposed Seronegative Women. *PloS One* (2020) 15(9):e0238347. doi: 10.1371/journal.pone.0238347
58. Cossarizza A, Ortolani C, Paganelli R, Barbieri D, Monti D, Sansoni P, et al. CD45 Isoforms Expression on CD4+ and CD8+ T Cells Throughout Life, From Newborns to Centenarians: Implications for T Cell Memory. *Mech Ageing Dev* (1996) 86(3):173–95. doi: 10.1016/0047-6374(95)01691-0
59. Saule P, Trauet J, Dutriez V, Lekeux V, Dessaint JP, Labalette M. Accumulation of Memory T Cells From Childhood to Old Age: Central and Effector Memory Cells in CD4(+) Versus Effector Memory and Terminally Differentiated Memory Cells in CD8(+) Compartment. *Mech Ageing Dev* (2006) 127(3):274–81. doi: 10.1016/j.mad.2005.11.001
60. Bradley T, Peppa D, Pedroza-Pacheco I, Li D, Cain DW, Henao R, et al. RAB11FIP5 Expression and Altered Natural Killer Cell Function Are Associated With Induction of HIV Broadly Neutralizing Antibody Responses. *Cell* (2018) 175387-399(2):e317. doi: 10.1016/j.cell.2018.08.064
61. Kestens L, Vanham G, Gigase P, Young G, Hannet I, Vanlangendonck F, et al. Expression of Activation Antigens, HLA-DR and CD38, on CD8 Lymphocytes During HIV-1 Infection. *AIDS* (1992) 6(8):793–7. doi: 10.1097/00002030-199208000-00004
62. Doisne JM, Urrutia A, Lacabaratz-Porret C, Goujard C, Meyer L, Chaix ML, et al. CD8+ T Cells Specific for EBV, Cytomegalovirus, and Influenza Virus Are Activated During Primary HIV Infection. *J Immunol* (2004) 173(4):2410–8. doi: 10.4049/jimmunol.173.4.2410
63. Papagno L, Spina CA, Marchant A, Salio M, Rufer N, Little S, et al. Immune Activation and CD8+ T-Cell Differentiation Towards Senescence in HIV-1 Infection. *PloS Biol* (2004) 2(2):E20. doi: 10.1371/journal.pbio.0020020
64. Sathaliyawala T, Kubota M, Yudanin N, Turner D, Camp P, Thome JJ, et al. Distribution and Compartmentalization of Human Circulating and Tissue-Resident Memory T Cell Subsets. *Immunity* (2013) 38(1):187–97. doi: 10.1016/j.immuni.2012.09.020
65. Baeyens A, Fang V, Chen C, Schwab SR. Exit Strategies: S1P Signaling and T Cell Migration. *Trends Immunol* (2015) 36(12):778–87. doi: 10.1016/j.it.2015.10.005
66. Kumar BV, Ma W, Miron M, Granot T, Guyer RS, Carpenter DJ, et al. Human Tissue-Resident Memory T Cells Are Defined by Core Transcriptional and Functional Signatures in Lymphoid and Mucosal Sites. *Cell Rep* (2017) 20(12):2921–34. doi: 10.1016/j.celrep.2017.08.078
67. Thome JJ, Yudanin N, Ohmura Y, Kubota M, Grinshpun B, Sathaliyawala T, et al. Spatial Map of Human T Cell Compartmentalization and Maintenance Over Decades of Life. *Cell* (2014) 159(4):814–28. doi: 10.1016/j.cell.2014.10.026
68. Cibrian D, Sanchez-Madrid F. CD69: From Activation Marker to Metabolic Gatekeeper. *Eur J Immunol* (2017) 47(6):946–53. doi: 10.1002/eji.201646837
69. Dogra P, Rancan C, Ma W, Toth M, Senda T, Carpenter DJ, et al. Tissue Determinants of Human NK Cell Development, Function, and Residence. *Cell* (2020) 180749-763(4):e713. doi: 10.1016/j.cell.2020.01.022
70. Kaech SM, Tan JT, Wherry EJ, Konieczny BT, Surh CD. Selective Expression of the Interleukin 7 Receptor Identifies Effector CD8 T Cells That Give Rise to Long-Lived Memory Cells. *Nat Immunol* (2003) 4(12):1191–8. doi: 10.1038/ni1009
71. Kondrack RM, Harbertson J, Tan JT, McBreen ME, Surh CD, Bradley LM. Interleukin 7 Regulates the Survival and Generation of Memory CD4 Cells. *J Exp Med* (2003) 198(12):1797–806. doi: 10.1084/jem.20030735
72. Moser JM, Gibbs J, Jensen PE, Lukacher AE. CD94-NKG2A Receptors Regulate Antiviral CD8(+) T Cell Responses. *Nat Immunol* (2002) 3(2):189–95. doi: 10.1038/ni757
73. Nattermann J, Feldmann G, Ahlenstiel G, Langhans B, Sauerbruch T, Spengler U. Surface Expression and Cytolytic Function of Natural Killer Cell Receptors is Altered in Chronic Hepatitis C. *Gut* (2006) 55(6):869–77. doi: 10.1136/gut.2005.076463
74. Sullivan LC, Nguyen THO, Harpur CM, Stankovic S, Kanagarajah AR, Koutsakos M, et al. Natural Killer Cell Receptors Regulate Responses of HLA-E-Restricted T Cells. *Sci Immunol* (2021) 6(58). doi: 10.1126/sciimmunol.abe9057

Conflict of Interest: The authors declare that the research was conducted in the absence of any commercial or financial relationships that could be construed as a potential conflict of interest.

Publisher's Note: All claims expressed in this article are solely those of the authors and do not necessarily represent those of their affiliated organizations, or those of the publisher, the editors and the reviewers. Any product that may be evaluated in this article, or claim that may be made by its manufacturer, is not guaranteed or endorsed by the publisher.